Biokinetic Characterization of the Acceleration Phase in Autotrophic Ammonia Oxidation

Kartik Chandran[1]*, Barth F. Smets[2]

ABSTRACT: Batch autotrophic ammonia oxidation tracked through oxygen uptake measurements displays a preliminary acceleration phase. Failure to recognize the acceleration phase and fitting batch ammonia oxidation profiles with standard Monod-type mathematical models can result in meaningless kinetic parameter estimates. The objectives of this study were to examine the factors controlling the acceleration phase and to derive and test empirical and metabolic models for its description. Because of possible sustained reducing power limitation during batch ammonia oxidation, the extent of the acceleration phase (1) increased with increasing initial ammonia concentration, (2) did not systematically vary with initial biomass concentrations, and (3) increased in response to starvation. Concurrent hydroxylamine oxidation significantly reduced the acceleration phase potentially by relieving reducing power limitation. A nonlinear empirical model described the acceleration phase more accurately than a linear empirical model. The metabolic model also captured experimental trends exceedingly well, but required determination of additional parameters and variables. *Water Environ. Res.*, **80,** 732 (2008).

KEYWORDS: acceleration phase, nitrification, biokinetics, extant respirometry, empirical and metabolic modeling.

doi:10.2175/106143008X296442

Introduction

The oxidation of ammonium-nitrogen (NH_4^+-N) to nitrite-nitrogen (NO_2^--N) serves as the primary source of energy for aerobic ammonium-nitrogen-oxidizing chemolithoautotrophic microorganisms. Ammonium-nitrogen is oxidized to hydroxylamine (NH_2OH) in the cytoplasm by ammonia monooxygenase (AMO). Hydroxylamine diffuses to the periplasm and is oxidized to NO_2^--N by hydroxylamine oxidoreductase (HAO) (Figure 1). The involvement of NH_2OH as a principal intermediate in NH_4^+-N oxidation has long been speculated (Lees, 1952) and is substantiated by its accumulation in small amounts in the presence of hydrazine (N_2H_4), an inhibitor of NH_2OH oxidation (Hofman and Lees, 1953). The oxidation of NH_4^+-N and NH_2OH are intimately linked; the reducing power generated in HAO-mediated NH_2OH oxidation is essential for AMO-driven NH_4^+-N oxidation. The electrons generated in NH_2OH oxidation are partially channeled to the terminal electron acceptor, oxygen, and partially back to AMO (Hooper et al., 1997). All the energy obtained by the ammonium-nitrogen-oxidizing bacteria is derived from the oxidation of NH_2OH to NO_2^--N (Hooper, 1989) and subsequent electron transfer phosphorylation.

A lag in NH_4^+-N oxidation has long been observed in batch studies with *Nitrosomonas europaea* and nitrifying enrichment cultures (Hooper, 1969; Suzuki and Kwok, 1981; Suzuki et al., 1981). During the lag period, the rate of NH_4^+-N oxidation accelerates from zero to a maximum rate. The acceleration is not captured in standard biokinetic models like the Monod expression, which could consequently result in meaningless parameter estimates describing autotrophic ammonia oxidation. While the initial acceleration phase has indeed been recognized, there have been no efforts at its mathematical characterization.

Based on the electron-mediated link between ammonia and hydroxylamine oxidation, we postulated that a minimum critical mass of NH_4^+-N needs to be processed before attainment of maximum specific activity, regardless of the initial NH_4^+-N concentration. We also postulated that the extent of the acceleration phase would increase with increasing ammonia-oxidizing biomass concentration in accordance with a specific reducing power requirement per cell. These postulates were challenged by defining the following objectives:

- To examine the experimental factors controlling the acceleration phase observed in NH_4^+-N oxidation, and
- To formulate and test empirical and mechanistic mathematical models to describe the acceleration phase.

Materials and Methods

Cultivation of a Nitrifying Enrichment Culture. A nitrifying enrichment consortium was grown and maintained in a 2-L sequencing batch reactor (SBR), operated at a hydraulic retention time of 1.25 days and a target solids retention time of 20 days. The details of reactor operation have been described previously (Chandran and Smets, 2000b). Upon attainment of steady-state, cell suspensions were periodically withdrawn from the reactor and used in respirometric tests.

Extant Respirometric Assay for Monitoring Nitrification Activity. The kinetics of NH_4^+-N oxidation were measured via extant respirometry (Chandran and Smets, 2000b; Ellis et al., 1996). Parallel respirometric assays were performed at 25°C in two 40-mL glass vessels according to a previously detailed procedure (Chandran and Smets, 2000b). Briefly, nitrifying cultures were withdrawn from the parent SBR just before the end of the react cycle and washed once by centrifugation at 4000 × g and resuspension in ammonia-free feed medium. The washed cell

[1] Department of Earth and Environmental Engineering, Columbia University, New York.

[2] Department of Environmental Engineering, DTU, Technical University of Denmark, Lyngby, Denmark.

* Department of Earth and Environmental Engineering, Columbia University, 500 West 120th Street, New York, NY 10027; e-mail: kc2288@columbia.edu.

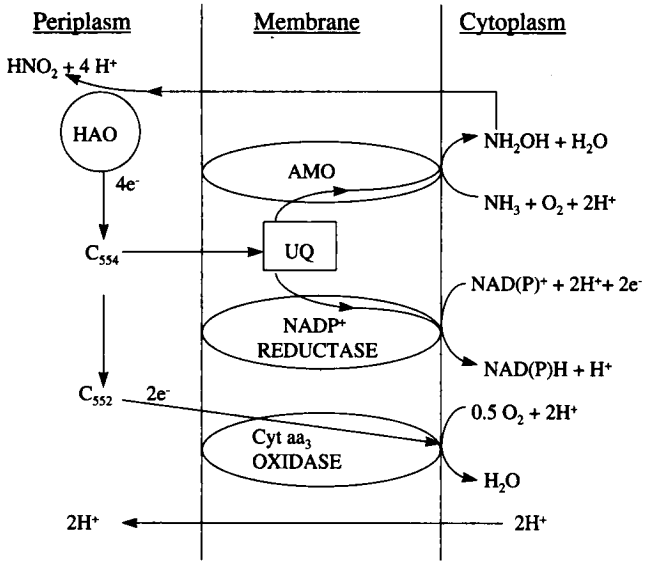

Figure 1—Electron transport in autotrophic ammonia oxidation (after Hooper, 1989).

suspensions were oxygenated with pure oxygen gas for 5 minutes and dispensed into two identical 40-mL glass respirometric vessels. The respirometric vessels were sealed with Clark-type dissolved oxygen (DO) electrodes (YSI 5331, YSI Inc., Yellow Springs, Ohio). The electrodes were connected to a dissolved oxygen monitor (YSI 5300, YSI Inc.) that was, in turn, connected to a personal computer via a data-acquisition interface. Dissolved oxygen readings were continuously acquired at a frequency of 4 Hz using indigenously developed virtual instruments written in LabView (National Instruments, Austin, Texas). After a 10-minute period of endogenous activity, respirometric assays were initiated by spiking the biomass with appropriate substrates (ammonia or hydroxylamine).

Substrate Solutions. Substrate solutions were freshly prepared before each set of respirometric assays, using laboratory-grade ammonium sulfate [$(NH_4)_2SO_4$] and hydroxylamine hydrochloride ($NH_2OH \cdot HCl$) (Fisher Scientific, Fair Lawn, New Jersey).

Nitrogen Analysis. The NH_4^+-N, NO_2^--N, and nitrate-nitrogen (NO_3^--N) were measured before and after the respirometric assays, according to *Standard Methods* (APHA et al., 2005). The NH_4^+-N was analyzed with an ammonia-gas-sensing electrode with an operating range of 7×10^{-3} to 1.4×10^4 mg NH_4^+-N/L (HNU Systems, Newton, Massachusetts). The NO_2^--N was assayed using a modification of the sulfanilic acid-N-naphthylethylenediamine addition method with an operating range of 5×10^{-3} to 1 mg-N/L. Nitrate-nitrogen was measured using a nitrate-ion-specific electrode (Corning Inc., Corning, New York) with an operating range of 1.4×10^{-2} to 1.4×10^4 mg NO_3^--N/L.

Convention for Expressing State Variables. We use a previously introduced convention to track state variables during respirometric nitrification assays by expressing reduced nitrogen species concentrations in terms of the nitrogenous oxygen demand (NOD), computed with respect to an appropriate reference nitrogen species (Chandran and Smets, 2001).

Determination of Biomass Concentrations. Biomass concentrations were measured as total chemical oxygen demand (tCOD) using commercially available reagents (Hach Company, Loveland, Colorado). Because the reactor influent was devoid of soluble COD, the ammonium-nitrogen-oxidizing biomass and nitrite-nitrogen-oxidizing biomass concentrations were approximated as being proportional to their respective biomass yield coefficients (Chandran and Smets, 2000a).

Mathematical Models for the Acceleration Phase in Ammonia Oxidation. The acceleration phase was modeled using an empirical approach and a metabolic approach. In the empirical approach, modified Monod expressions were developed that considered transient changes in the apparent μ_{max}. A linear relationship between transient apparent μ_{max} and oxygen consumption was initially considered. In this approach, μ_{max} increases linearly from zero at the point of substrate injection to the true μ_{max} at the end of the acceleration phase (eq 1). The end of the acceleration phase is defined by a critical dissolved oxygen concentration, DO_c, after which, maximal activity ensues (Figures 2a and 2b). Using respirometric data, DO_c can easily be identified from dissolved oxygen versus time or oxygen uptake rate versus dissolved oxygen profiles at the point of peak oxygen uptake rate activity (Figures 2a and 2b). The oxygen consumed during the acceleration phase, ΔDO_c, was calculated from the difference between the dissolved oxygen concentration at the point of substrate injection (DO_i) and DO_c. The ΔDO_c can stoichiometrically be related to NH_4^+-N consumed during the acceleration phase, as per Smets et al. (1996). Because of the poor descriptive ability of eq 1, a nonlinear model was also formulated. In this approach, μ_{max} is nonlinearly related to the ratio of instantaneous oxygen uptake in the acceleration phase to ΔDO_c, given by $[(DO\text{-}DO_c)/\Delta DO_c]$, using an exponent n (eq 2). In formulating the empirical models, we assumed that NH_4^+-N oxidation, biomass growth, and oxygen uptake are linked by the same stoichiometry during and after the acceleration phase. Units for all equations are defined in Table 1.

$$\mu = \mu_{max,ns}[1 - k(DO - DO_C)] * \frac{S_{nh} * X_{ns}}{K_{S,ns} + S_{nh}} \text{ at } DO > DO_c, \text{ or}$$

$$\mu = \mu_{max,ns} * \frac{S_{nh} * X_{ns}}{K_{S,ns} + S_{nh}} \quad (1)$$

$$\mu = \mu_{max,ns}\left[1 - \left(\frac{DO - DO_c}{DO_i - DO_c}\right)^n\right] * \frac{S_{nh} * X_{ns}}{K_{S,ns} + S_{nh}} \text{ at } DO > DO_c, \text{ or}$$

$$\mu = \mu_{max,ns} * \frac{S_{nh} * X_{ns}}{K_{S,ns} + S_{nh}} \quad (2)$$

Equations 1 and 2 contain one parameter, k or n, in addition to the Monod coefficients $\mu_{max,ns}$ and $K_{S,ns}$ to be estimated. The DO_c was obtained directly from the d(DO)/dt versus DO profile (i.e., Figure 2b) and was treated as a constant in subsequent parameter estimation.

Parameter Estimation of Empirical Models. Differential equations representing nitrogen removal, oxygen uptake, and biomass synthesis have been derived earlier and are summarized here in a matrix format (Table 2) (Chandran and Smets, 2000a). Differential equations for each species can be obtained by multiplying the kinetic terms in the last column of Table 2 with the appropriate stoichiometric term in columns 2 through 5. Biokinetic parameters for experimental respirograms fit to equations shown in Table 2, and modified Monod expressions (eqs 1 and 2) were estimated by minimizing the sum of the squared errors (SSE) between the experimental and predicted cumulative oxygen uptake data, using the SOLVER utility in Microsoft Excel (Microsoft Corporation, Redmond, Washington). The maximum specific activity associated with the ammonium-nitrogen-oxidizing biomass fractions was expressed in terms of the maximum specific substrate consumption rate (Chandran and Smets, 2000b).

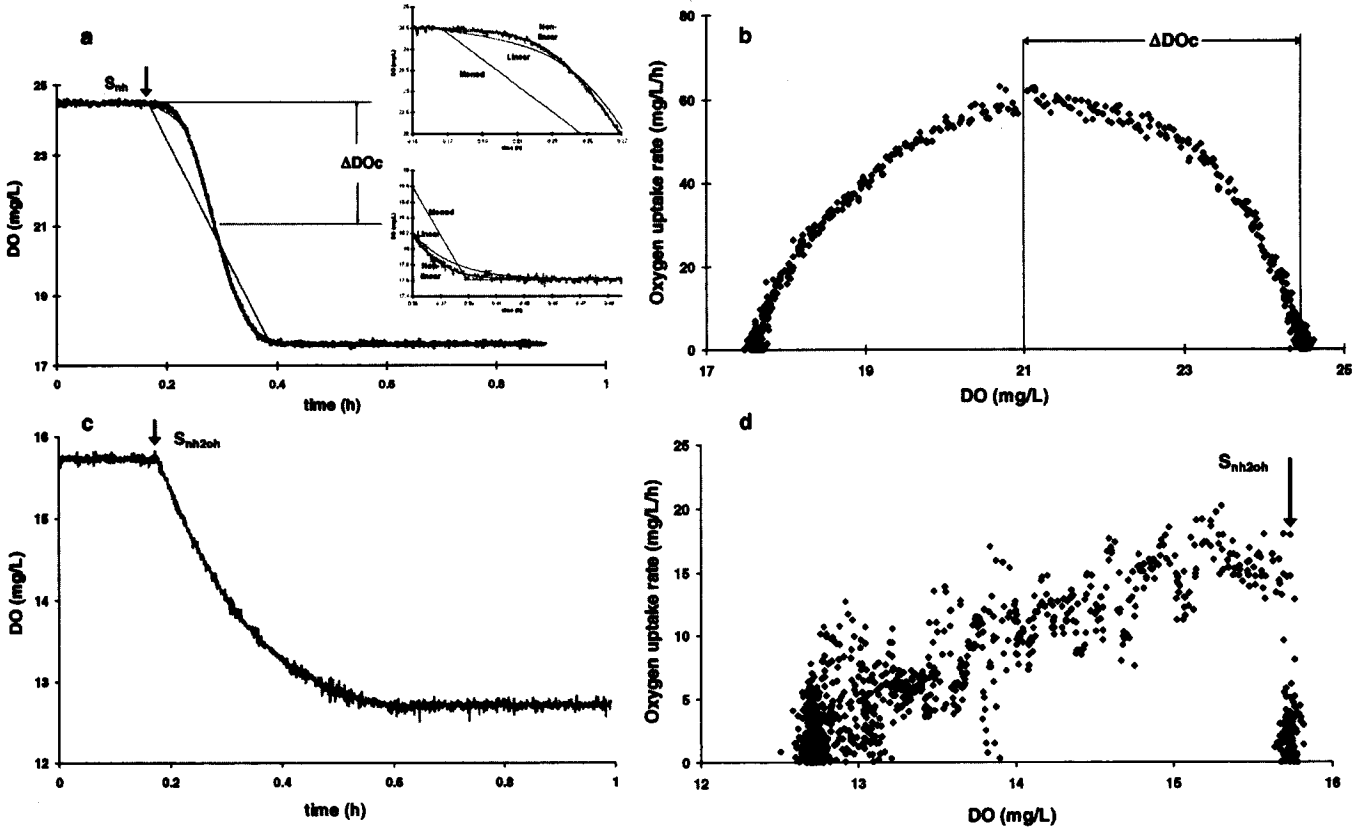

Figure 2—Simulation of the acceleration phase by different models. Solid lines are experimental data and best-fit profiles, respectively. Insets amplify respirogram regions of highest μ_{max} and K_S sensitivity (panel a). Acceleration is also reflected in the oxygen uptake rate profile (panel b). $S_{nh,o}$ = 7.7 mg NOD/L, $X_{ns,o}$ = 397 mg COD/L. Absence of a lag in NH_2OH oxidation is reflected in cumulative oxygen uptake (panel c) and oxygen uptake rate (panel d) profiles. $S_{nh,o}$ = 6.9 mg NOD/L, $X_{ns,o}$ = 397 mg COD/L.

In the metabolic approach to modeling the acceleration phase transient, a set of additional differential equations were formulated that explicitly consider the link between NH_4^+-N and NH_2OH oxidation, focusing on generation and use of reducing equivalents (eqs 3 to 8).

$$NH_3 + AH_2 + O_2 \rightarrow NH_2OH + H_2O + A \quad (3)$$

$$NH_2OH + A + 0.5\ O_2 \rightarrow HNO_2 + AH_2 \quad (4)$$

Equation 4 represents all the downstream reactions of NH_2OH oxidation, that is, both oxygen reduction and transfer of electrons to internal reducing power. Assuming that the enzymatic transformations display a Michaelis-Menten dependence on their substrates, the following molar-based governing equations can be derived.

$$\frac{dS_{nh}}{dt} = -k_{amo}\frac{S_{nh}}{K_{S,nh}+S_{nh}}\frac{S_{ah2}}{K_{S,ah2}+S_{ah2}}X_{amo} \quad (5)$$

$$\frac{dS_{nh2oh}}{dt} = k_{amo}\frac{S_{nh}}{K_{S,nh}+S_{nh}}\frac{S_{ah2}}{K_{S,ah2}+S_{ah2}}X_{amo} - k_{hao}\frac{S_{nh2oh}}{K_{S,nh2oh}+S_{nh2oh}}X_{hao} \quad (6)$$

$$\frac{dS_{ah2}}{dt} = -k_{amo}\frac{S_{nh}}{K_{S,nh}+S_{nh}}\frac{S_{ah2}}{K_{S,ah2}+S_{ah2}}X_{amo} + 2 * k_{hao}\frac{S_{nh2oh}}{K_{S,nh2oh}+S_{nh2oh}}X_{hao} \quad (7)$$

$$\frac{dS_{O2}}{dt} = -k_{amo}\frac{S_{nh}}{K_{S,nh}+S_{nh}}\frac{S_{ah2}}{K_{S,ah2}+S_{ah2}}X_{amo} - 0.5 * f_{O_2} * k_{hao}\frac{S_{nh2oh}}{K_{S,nh2oh}+S_{nh2oh}}X_{hao} \quad (8)$$

Values for AMO and HAO concentrations (X_{amo} and X_{hao}, respectively, mmol/L) were adjusted to match the duration of the simulated NH_4^+-N oxidation respirogram (eqs 5 to 8) with typical experimental respirograms, which lasted approximately 30 minutes from NH_4^+-N injection to exhaustion. Further, concentrations and half-saturation constants for reducing power, AH_2 and $K_{S,ah2}$, respectively, and concentrations of X_{amo} and X_{hao} were also expressed in molar units, because their oxygen equivalency was not known. Consequently, the units for the maximum specific rate constants, k_{amo} and k_{hao} were expressed as milligrams NOD per millimole per hour. Concentrations and half-saturation constants for ammonia and hydroxylamine were expressed in terms of the NOD convention to be consistent with empirical model terminology. Significantly, eq 8 recognizes that energy generation via respiratory consumption of oxygen is only associated with NH_2OH oxidation and not directly with NH_4^+-N oxidation (Hooper, 1989). Only a fraction of this available energy is used (f_{O2}), as the other electrons are used in metabolic carbon dioxide fixation. The differential equations were simultaneously solved using Polymath 6.0 (Polymath Software, Willimantic, Connecticut), to give time

Table 1—Definitions and units for variables.*

Symbol	Definition	Units in empirical models	Units in metabolic model
S_{nh}	NH_4^+-N concentration	mg NOD/L	mg NOD/L
S_{no2}	NO_2^--N concentration	mg NOD/L	NA
S_{nh2oh}	NH_2OH concentration	NA	mg NOD/L
S_{o2}	Dissolved oxygen concentration	mg O_2/L	mg O_2/L
S_{ah2}	Reducing equivalents in reduced state	NA	mmol/L
X	Biomass concentration	mg COD/L	mg COD/L
μ_{max}	Maximum specific growth rate	1/hour	NA
K_S	Half-saturation coefficient	mg NOD/L	mg NOD/L
q_{max}	Maximum specific substrate consumption rate	mg NOD/mg COD/h	NA
f_S	Fraction of available electrons used in biomass synthesis	unitless	NA
Ou	Oxygen uptake	mg O_2/L	mg O_2/L
k	Additional parameter in linear empirical model	L/mg O_2	NA
n	Additional parameter in nonlinear empirical model	unitless	NA
DO_C	Critical dissolved oxygen concentration at which maximum NH_4^+-N oxidation commences	mg O_2/L	NA
ΔDO_C	Cumulative oxygen consumption during the acceleration phase	mg O_2/L	mg O_2/L
t	Time	hours	hours
k_{amo}	Maximum specific NH_4^+-N oxidation rate by AMO	NA	mg NOD/mmol-X_{amo}/h
X_{amo}	Initial AMO concentration	NA	mmol/L
$K_{S,nh}$	Half-saturation coefficient of AMO for NH_4^+-N	NA	mg NOD/L
k_{hao}	Maximum specific NH_2OH oxidation rate by HAO	NA	mg NOD/mmol-X_{hao}/h
X_{hao}	Initial HAO concentration	NA	mmol/L
$K_{S,nh2oh}$	Half-saturation coefficient of HAO for NH_2OH	NA	mg NOD/L
f_{O2}	Fraction of available electrons in NH_2OH oxidation channeled to oxygen	NA	unitless
$K_{S,ah2}$	Half-saturation coefficient for AH_2	NA	mmol/L

* Notes: NA signifies that the symbol was not used in a given model; subscript ns denotes NH_4^+-N to NO_2^--N oxidation; subscript nb denotes NO_2^--N to NO_3^--N oxidation; A = oxidized form of reducing equivalents (mmol/L); and AH_2 = reduced form of reducing equivalents (mmol/L).

series profiles of NH_4^+-N, NH_2OH, AH_2, and O_2. Using the model and parameter estimates (Table 3), different initial NH_4^+-N and biomass concentrations (via proportional changes in X_{amo} and X_{hao}) were considered, and their conceptual effect on the extent of the acceleration phase was checked via model simulations. The model was also used to verify the effect of sequential pulses of NH_2OH and NH_4^+-N on the extent of the acceleration phase.

Results

Hydroxylamine Oxidation. There was no discernible acceleration associated with the oxidation of NH_2OH (Figures 2c and 2d). Further, as expected, the cumulative oxygen uptake observed in the NH_2OH oxidation assays suggested that not all 4 electrons available from the oxidation of NH_2OH to NO_2^--N were transferred to O_2, the terminal electron acceptor. According to Figure 1, only two of the four electrons available from NH_2OH to NO_2^--N oxidation are transferred to O_2, corresponding to a 50% recovery. The corresponding electron recovery during NH_2OH to NO_3^--N oxidation is 67%, assuming that all the electrons from NO_2^--N oxidation are recovered on O_2. Experimentally observed electron recoveries on O_2 of 61 ± 22% (n = 3) and 68 ± 13% (n = 6) for NH_4^+-N to NO_2^--N oxidation and NH_2OH to NO_3^--N oxidation, respectively (data not shown) (Chandran, 1999), suggested congruence with theoretical expectations.

Effect of Initial Ammonia Concentration on the Acceleration Phase. In extant assays conducted with initial NH_4^+-N concentrations in the range 3 to 12 mg NOD/L and constant biomass concentrations (432 ± 5 mg COD/L), the extent of the acceleration phase, measured by ΔDO_c, increased with increasing NH_4^+-N concentrations (Figure 3a). Additionally, the fractional oxygen or alternately fractional NH_4^+-N consumption during the acceleration phase ($\Delta DO_C/OU_f$) was constant, irrespective of $S_{nh,o}$ (Figure 3c).

Effect of Biomass Concentration and Specific Activity on the Acceleration Phase. At 6 biomass concentrations tested in the

Table 2—Elements of a mechanistic nitrification model used to describe nitrification respirograms (Chandran and Smets, 2000a). Description and units for state variables are provided in the Nomenclature section.

State variable	S_{nh}	S_{no2}	Ou_{ns}	Ou_{nb}	X_{ns}	X_{nb}	Rate expression
ns	$-\frac{(1+(0.3*f_{S,ns}))}{f_{S,ns}}$	$+\frac{1}{3*f_{S,ns}}$	$+\frac{(1-f_{S,ns})}{f_{S,ns}}$		+1		$\mu_{max,ns} * \frac{X_{ns}*Snh}{K_{S,ns}+S_{nh}}$
nb		$-\frac{1}{f_{S,nb}}$		$+\frac{(1-f_{S,nb})}{f_{S,nb}}$		+1	$\mu_{max,nb} * \frac{X_{nb}*S_{no2}}{K_{S,nb}+S_{no2}}$

range 200 to 2500 mg COD/L, at relatively uniform $S_{nh,o}$ values of 6.2 ± 0.7 mg NOD/L, ΔDO_c values decreased slightly with increasing biomass concentration (Figure 3e, symbol ◆). The effect of prolonged endogenous respiration on the extent of acceleration was investigated by overnight aeration with laboratory air of a biomass sample in the absence of exogenous electron donors, before resuming NH_4^+-N dosing. The acceleration phase markedly increased after extended endogenous activity (Figure 3e, symbol ■). In this case, although the total biomass concentration was constant, the specific activity decreased, which led to an extension of the acceleration period.

Effect of Prior Ammonia or Hydroxylamine Oxidation on the Acceleration Phase. There was no discernible effect of prior NH_4^+-N oxidation on ΔDO_c, based on extant respirometric assays conducted with biomass samples exposed to a series of NH_4^+-N pulses. For a representative set of respirograms describing NH_4^+-N to NO_2^--N oxidation, ΔDO_c values of 2.5, 2.4, and 2.9 mg/L were observed for three sequential NH_4^+-N injections. Prior NH_2OH oxidation also did not affect the extent of the acceleration phase. For a representative set of respirometric assays, an NH_4^+-N injection preceded by an NH_2OH injection resulted in a ΔDO_c of 3.1 mg/L, as opposed to a ΔDO_c of 3 mg/L for an NH_4^+-N injection preceded by an NH_4^+-N injection (data not shown).

Effect of Simultaneous Hydroxylamine and Ammonia Oxidation on the Acceleration Phase. When respirometric assays were initiated with an NH_2OH injection, and an additional pulse of NH_4^+-N was applied before the complete exhaustion of the added NH_2OH, the extent of the acceleration phase was significantly reduced (Figure 4a).

Acceleration Phase Modeling. *Empirical Models for Describing the Acceleration Phase.* The acceleration phase in NH_4^+-N oxidation could not be described using standard Monod kinetics [SSE = 229. 8 $(mg/L)^2$, Figure 2a]. The linear model (eq 1) was also inadequate in describing the oxygen uptake profile during the initial acceleration phase with either k alone or both k and DO_c as parameters to be estimated (data not shown). The nonlinear model provided a better description of the acceleration phase than the linear model [SSE 1.58 versus 5.76 $(mg/L)^2$, Figure 2a].

Because of their empirical nature, it is not possible to interpret the superiority of the nonlinear model over the linear model from a fundamental mechanistic perspective. This was the primary motivation for developing the mechanistic metabolic model in this study, which explicitly implicates reducing power limitation as a primary cause for the existence of the acceleration phase.

Simulation-Based Evaluation of the Role of Reducing Power on the Acceleration Phase. The more detailed metabolic model allowed us to track the kinetics of NH_4^+-N, NH_2OH, and AH_2 during batch ammonia oxidation and capture the transients in these species well (Figures 5a and 5b). Significantly, the model predictions matched the effects on the acceleration phase that were observed when modifying experimental variables like X_o and S_o (Figure 3). The simulations predicted the following:

(1) An increase in ΔDO_c with increasing $S_{nh,o}$ (Figure 3b),
(2) A slightly increasing ratio of $\Delta DOC/OU_f$ with increasing $S_{nh,o}$ (Figure 3d),
(3) A relatively minor change in ΔDO_c with increasing X_o (Figure 3f), and
(4) A near-complete reduction of the acceleration phase during concurrent NH_4^+-N and NH_2OH oxidation (Figure 4b).

Table 3—Parameters used for the metabolic model for acceleration phase.

Symbol (units)	Value	Reference
k_{amo} (mg NOD/mmol-X_{amo}/h)	144	Calculated from Chandran and Smets (2000a)[a]
X_{amo} (mmol/L)	5	[b]
$K_{S,nh}$ (mg NOD/L)	1.68	Chandran and Smets (2000a)
k_{hao} (mg NOD/mmol-X_{amo}/h)	144	Assumed equal to k_{amo}
X_{hao} (mmol/L)	5	[b]
$K_{S,nh2oh}$ (mmol/L)	11.2	Assumed
f_{O2}	0.5	Electron transport scheme for NH_4^+-N oxidation (Hooper, 1989)
$K_{S,ah2}$ (mmol/L)	0.35	Assumed

[a] Maximum specific growth rate value of 0.95 mg NOD/mg COD/h converted to mmol-S_{nh}/mmol-X_{amo}/h, assuming 1 mole X_{amo} per mole ammonia-oxidizing bacteria.
[b] Adjusted so simulated respirograms match typical experimental NH_4^+-N oxidation respirograms (Chandran, 1999).

Discussion

Hypotheses for the Existence of an Acceleration Process. Our experimental and metabolic model simulation results strongly suggest that the fundamental coupling between NH_4^+-N and NH_2OH oxidation results in the acceleration phase in batch NH_4^+-N oxidation respirograms. However, several alternate phenomena could possibly contribute to the observed acceleration phase. Under a slow signal response of dissolved oxygen electrodes, an acceleration phase can be expected in the respirograms for all substrates. However, because the acceleration phase was not experimentally observed in NH_2OH or NO_2^--N oxidation respirograms (Chandran, 1999), the contribution of a slow dissolved oxygen electrode response to the acceleration phase can be rejected. Substrate inhibition by NH_4^+-N could also result in an initial curvature in batch NH_4^+-N oxidation respirograms. However, the initial concentrations at which our experiments were performed (approximately 4 mg NH_4^+-N/L) are far below the self-inhibitory concentrations for autotrophic ammonia oxidation (Anthonisen et al., 1976). Therefore, substrate inhibition does not contribute to the acceleration phase in our respirograms. Starvation and parallel transient accumulation of NH_4^+-N and NH_2OH could also lead to an acceleration-type phenomenon in both NH_4^+-N and NH_2OH oxidation (Schmidt et al., 2004). However, we rule out starvation as a determinant phenomenon in our experiments. In general, respirometric assays were conducted within 30 minutes (typically 15 minutes) after the biomass was harvested from the parent SBR, just before the end of the 6-hour react cycle. Additionally, no acceleration phase was noted in NH_2OH oxidation respirograms from similarly processed biomass samples.

Effect of Initial Ammonia and Biomass Concentrations on the Acceleration Phase. The increase in ΔDO_c with increasing $S_{nh,o}$ (Figure 3a) and the constant value of the $\Delta DO_c/OU_f$ ratio (Figure 3c) violated the hypothesis that the extent of the acceleration phase should be independent of the initial NH_4^+-N concentration. In our hypothesis, we assumed that, during the batch respirometric assay, the limitation in reducing power is relieved sometime during the assay. However, for the parameter set used, simulations using the metabolic model showed sustained reducing

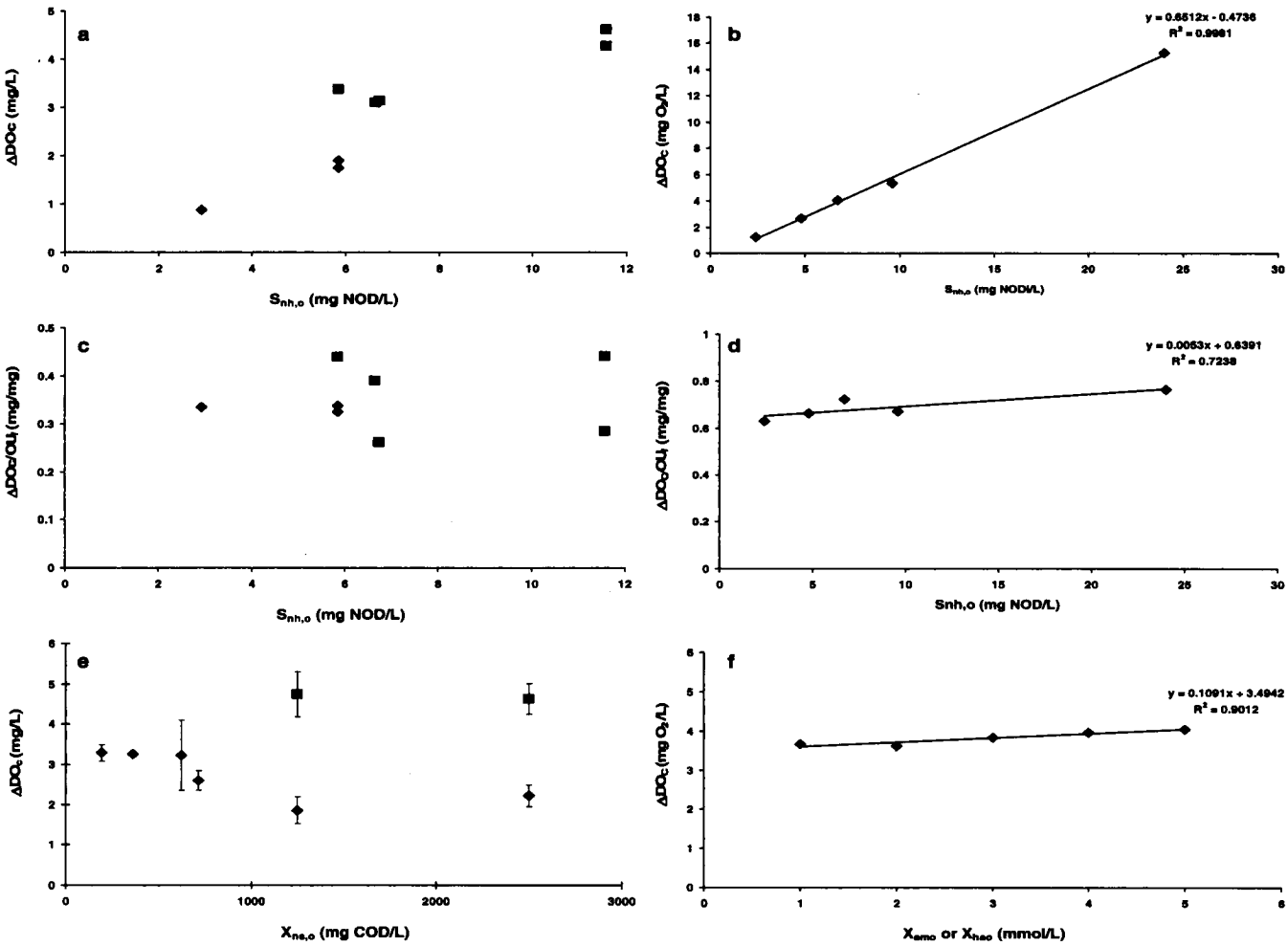

Figure 3—Effect of $S_{nh,o}$ on ΔDO_c (panel a) and $\Delta DO_c/OU_f$ (panel c) for respirometric assays conducted on different days, (◆, ■), $X_{ns,o}$ = 432 ± 5 mg *X* COD/L. Effect of $X_{ns,o}$ on ΔDO_c at *t* = 1 hour (◆) and *t* = 12 hours (■) after removal of biomass from the parent SBR, $S_{nh,o}$ = 6.2 ± 0.7 mg NOD/L (panel c). Simulations from the metabolic model (panels b, d, and f) show trends similar to experimental results. Straight lines are obtained from linear regression with accompanying equation and regression coefficient. Initial conditions were $X_{amo} = X_{hao}$ = 5 mmol/L (panels b and d) and $S_{nh,o}$ = 6.72 mM (panel f).

power limitation during the entire assay ($S_{ah2,\ max} = 0.15 < K_{S,ah2} = 0.35$, Figure 5b). With sustained reducing power limitation determining the overall rate of ammonia oxidation, $S_{nh,o}$ or X_o are not expected to affect the extent of the acceleration phase, and a fixed value of $\Delta DO_C/OU_f$ would indeed be observed, consistent with experimental results. Therefore, in accordance with the metabolic model simulations, sustained reducing power limitation during the respirometric assays could have possibly resulted in the experimentally observed effects of $S_{nh,o}$ and X_o on ΔDO_c. On the other hand, the increased acceleration phase after overnight aeration without substrate may be attributed to a loss in *amo* mRNA transcript abundance and ammonia-oxidation activity in response to a relatively longer starvation phase (Bollmann et al., 2005; Chandran and Love, 2008; Stein and Arp, 1998; Wei et al., 2006) and the coupling between AMO and HAO.

Effect of Ammonia and Hydroxylamine Oxidation on the Acceleration Phase. The fundamental coupling between NH_4^+-N and NH_2OH oxidation (Figure 1) was strikingly demonstrated by substantial reduction of the acceleration phase during the concomitant oxidation of NH_4^+-N and NH_2OH (Figures 4a and 4b). Similar reduction of the acceleration phase has been reported in the presence of small amounts of NH_2OH (Hooper, 1969). In contrast to earlier reports (Hooper, 1969), prior oxidation of NH_4^+-N or NH_2OH failed to shorten the acceleration phase, possibly because of sustained reducing power limitation during the batch respirometric assays.

Mathematical Modeling and Parameter Estimation of the Acceleration Phase in Ammonia Oxidation. The principal assumption made in using the Monod expression to describe batch respirograms is that the biomass shifts from an endogenous state to a peak respiration phase immediately upon exposure to an exogenously added substrate. Consequently, the unmodified Monod expression is applicable only if the acceleration phase is truncated and not considered while modeling the NH_4^+-N oxidation respirograms. However, such truncation results in underestimates of both the maximum specific activity and the half-saturation coefficient of NH_4^+-N oxidation and introduces considerable subjectivity into the parameter estimates. Thus, an accurate portrayal of the acceleration

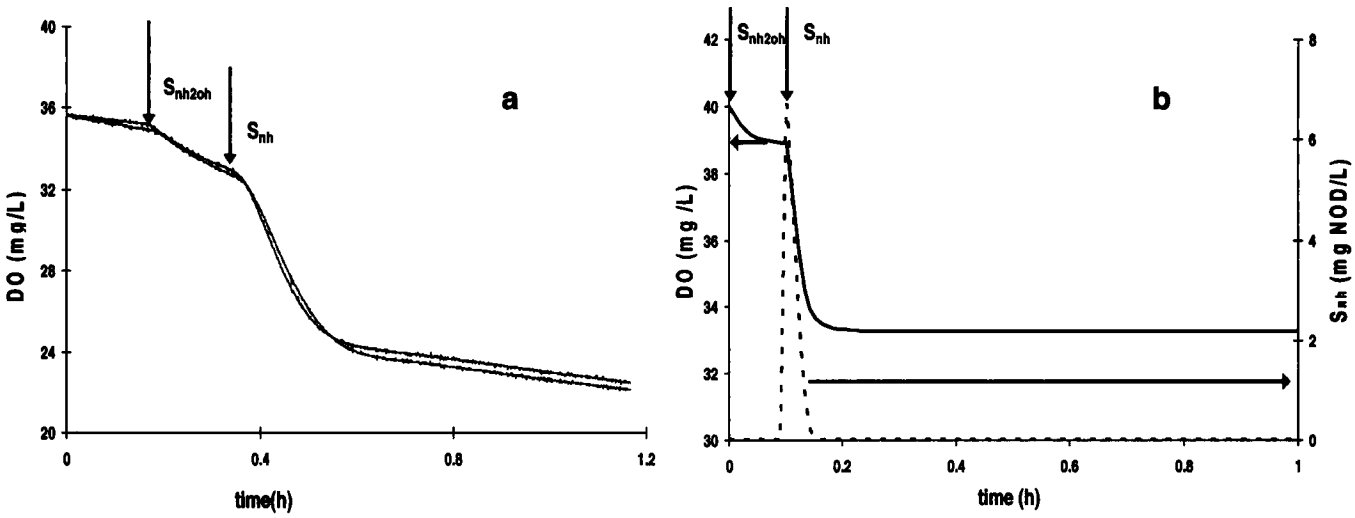

Figure 4—Significant reduction of the acceleration phase by concomitant oxidation of NH_2OH and NH_4^+-N in duplicate experiments (panel a) and metabolic model simulations (panel b).

phase is mandatory to avoid erroneous kinetic parameter estimates describing NH_4^+-N oxidation. The explicit mathematical treatment of the acceleration phase in NH_4^+-N oxidation presented in this work represents a significant improvement beyond the arbitrary truncation approach.

Another important outcome of our work is the metabolic model concept for describing the acceleration phase. The conceptual metabolic model provided good agreement and explanations for experimental trends in the acceleration phase as a function of initial substrate and biomass concentrations and the effect of concurrent hydroxylamine and ammonia oxidation. Indeed, the application of the metabolic model in conjunction with measurements of intracellular reducing power could potentially lead to a thorough characterization of the acceleration phase in autotrophic ammonia oxidation. Autotrophic ammonia-oxidizing bacteria, such as *N. europaea*, are thought to be especially susceptible to oxidative stressors that deplete intracellular reserves of reducing power (Chain et al., 2003). We have also recently shown that cultures of *N. europaea* are subject to oxidative stress by a diverse array of inhibitory compounds, including heavy metals (cadmium) and chlorine-based disinfectants (Chandran and Love, 2008; Vikesland et al., 2007). Therefore, the development and future application of intracellular reducing power measurements in conjunction with our metabolic model can be used to gain mechanistic insights to inhibition of nitrification also.

Conclusions

In this study, we examined factors that contribute to the acceleration phase in batch NH_4^+-N oxidation respirograms and developed models for its description. Our experimental results and metabolic model simulations both supported the reducing-power-based coupling between NH_4^+-N and NH_2OH oxidation. The acceleration phase was largely eliminated by concomitant oxidation of NH_4^+-N and NH_2OH. Our results show that, as a result of sustained reducing power limitation during batch respirometric assays, the extent of the acceleration phase increased with initial

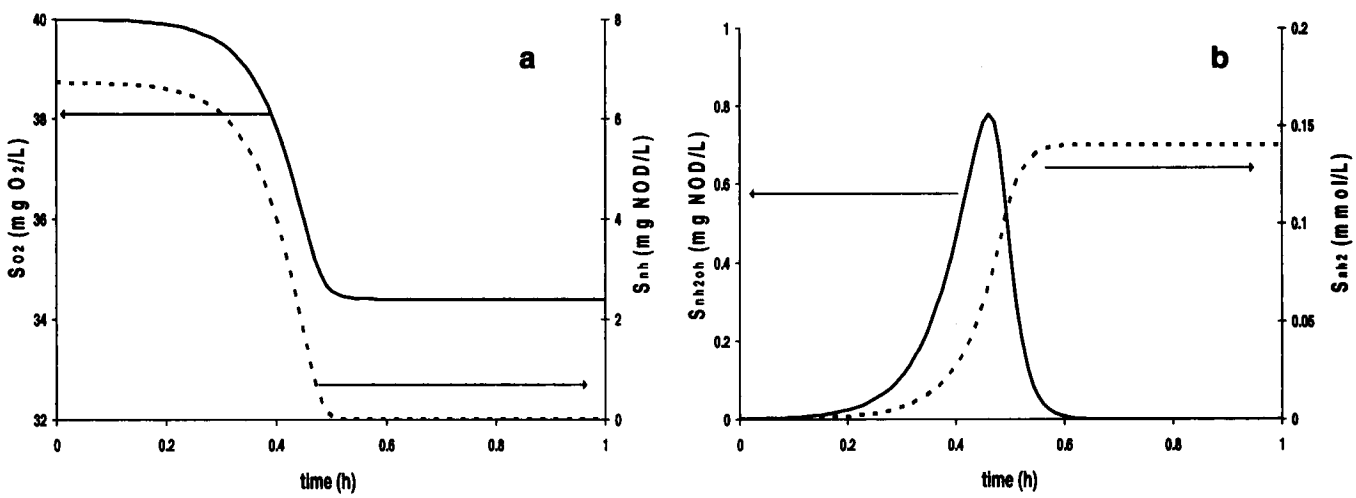

Figure 5—Simulated profiles of S_{nh} (dashed line) and S_{o2} (solid line) (panel a) and S_{nh2oh} and S_{ah2} (panel b) using the metabolic model.

NH_4^+-N concentrations, and a fixed fraction of the initial NH_4^+-N was processed during the acceleration phase. The acceleration phase was minimally affected by the biomass concentrations in the range tested, but increased after overnight endogenous respiration. Of the two empirical models formulated, the nonlinear model provided a better representation of the acceleration than the linear model. The metabolic modeling approach yielded trends consistent with experimental results and merits further use in conjunction with explicit future measurements of intracellular reducing power.

Credits

Part of this paper was presented at the Leading Edge Research Symposium during the *77th Annual Water Environment Federation Technical Exposition and Conference* (2004). The metabolic modeling aspect of this paper is a new development and has not been published or presented elsewhere.

Submitted for publication September 20, 2007; revised manuscript submitted March 3, 2008; accepted for publication March 13, 2008.

The deadline to submit Discussions of this paper is November 15, 2008.

References

American Public Health Association; American Water Works Association; Water Environment Federation (2005) *Standard Methods for the Examination of Water and Wastewater,* 21st ed.; American Public Health Association: Washington, D.C.

Anthonisen, A. C.; Loehr, R. C.; Prakasam, T. B. S.; Srinath, E. G. (1976) Inhibition of Nitrification by Ammonia and Nitrous Acid. *J. Water Pollut. Control Fed.,* **48,** 835–852.

Bollmann, A.; Schmidt, I.; Saunders, A. M.; Nicolaisen, M. H. (2005) Influence of Starvation on Potential Ammonia-Oxidizing Activity and *amoA* mRNA Levels of *Nitrosospira briensis*. *Appl. Environ. Microbiol.,* **71,** 1276–1282.

Chain, P.; Lamerdin, J.; Larimer, F.; Regala, W.; Lao, V.; Land, M.; Hauser, L.; Hooper, A.; Klotz, M.; Norton, J.; et al. (2003) Complete Genome Sequence of the Ammonia-Oxidizing Bacterium and Obligate Chemolithoautotroph *Nitrosomonas europaea*. *J. Bacteriol.,* **185,** 2759–2773.

Chandran, K. (1999) Biokinetic Characterization of Ammonia and Nitrite Oxidation by a Mixed Nitrifying Culture Using Extant Respirometry. Ph.D. Dissertation, University of Connecticut, Storrs.

Chandran, K.; Love, N. G. (2008) Physiological State, Growth Mode and Oxidative Stress Play a Role in Cd(II)-Mediated Inhibition of *Nitrosomonas europaea* 19718. *Appl. Environ. Microbiol.* **74,** 2447–2453.

Chandran, K., Smets, B. F. (2000a) Applicability of two-step models in estimating nitrification kinetics from batch respirograms under different relative dynamics of ammonia and nitrite oxidation. *Biotechnol. Bioeng.,* **70,** 54–64.

Chandran, K.; Smets, B. F. (2001) Estimating Biomass Yield Coefficients for Autotrophic Ammonia and Nitrite Oxidation from Batch Respirograms. *Water Res.,* **35,** 3153–3156.

Chandran, K.; Smets, B. F. (2000b) Single-Step Nitrification Models Erroneously Describe Batch Ammonia Oxidation Profiles When Nitrite Oxidation Becomes Rate Limiting. *Biotechnol. Bioeng.,* **68,** 396–406.

Ellis, T. G.; Barbeau, D. S.; Smets, B. F.; Grady, C. P. L. J. (1996) Respirometric Technique for Determination of Extant Kinetic Parameters Describing Biodegradation. *Water Environ. Res.,* **68,** 917–926.

Hofman, T.; Lees, H. (1953) The Biochemistry of the Nitrifying Organisms. 4: The Respiration and Intermediary Metabolism of *Nitrosomonas*. *Biochem. J.,* **54,** 579–583.

Hooper, A. B. (1989) Biochemistry of the Nitrifying Lithoautotrophic Bacteria. In *Autotrophic Bacteria,* Schlegel, H. G., Bowien, B. (Eds); Springer-Verlag: Berlin, Germany.

Hooper, A. B. (1969) Lag Phase of Ammonia Oxidation by Resting Cells of *Nitrosomonas europaea*. *J. Bacteriol.,* **97,** 968–969.

Hooper, A. B.; Vannelli, T.; Bergmann, D. J.; Arciero, D. M. (1997) Enzymology of the Oxidation of Ammonia to Nitrite by Bacteria. *Antonie van Leeuwenhoek,* **71,** 59–67.

Lees, H. (1952) Hydroxylamine as an Intermediate in Nitrification. *Nature (London),* **169,** 156–157.

Schmidt, I.; Look, C.; Bock, E.; Jetten, M. S. M. (2004) Ammonium and Hydroxylamine Uptake and Accumulation in Nitrosomonas. *Microbiol.,* **150,** 1405–1412.

Smets, B. F.; Jobbágy, A.; Cowan, R. M.; Grady, C. P. L. J. (1996) Evaluation of Respirometric Data: Identification of Features that Preclude Data Fitting with Existing Kinetic Expressions. *Ecotoxicol. Environ. Saf.,* **33,** 88–99.

Stein, L. Y.; Arp, D. J. (1998) Loss of Ammonia Monooxygenase Activity in *Nitrosomonas europaea* Upon Exposure to Nitrite. *Appl. Environ. Microbiol.,* **64,** 4098–4102.

Suzuki, I.; Kwok, S. C. (1981) A Partial Resolution and Reconstitution of the Ammonia-Oxidizing System in *Nitrosomonas europaea*: Role of Cytochrome c_{554}. *Can. J. Biochem.,* **59,** 484–488.

Suzuki, I.; Kwok, S. C.; Dular, U.; Tsang, D. C. Y. (1981) Cell-Free Ammonia Oxidizing System of *Nitrosomonas europaea*: General Conditions and Properties. *Can. J. Biochem.,* **59,** 477–483.

Vikesland, P. J.; Digiano, F. A.; Love, N. G.; Chandran, K.; Ferguson, B.; Fiss, E. M.; Rebodos, R.; Zaklikowski, A. E. (2007) Seasonal Chlorination Practices and Impacts to Chloraminating Utilities. AWWA Research Foundation: Denver, Colorado.

Wei, X.; Yan, T.; Hommes, N. G.; Liu, X.; Wu, L.; McAlvin, C.; Klotz, M. G.; Sayavedra-Soto, L. A.; Zhou, J.; Arp, D. J. (2006) Transcript Profiles of *Nitrosomonas europaea* During Growth and Upon Deprivation of Ammonia and Carbonate. *FEMS Microbiol. Lett.,* **257,** 76–83.